

RESEARCH PAPER

Study of the Structural Properties of Rhodamine Dye-Doped With TiO₂ Nanoparticles

Noor Al-Huda A. Rwayyih, Khawla J. Tahir *, Noor J. Ridha, Firas K. Mohamad Alosfur

Department of Physics, College of Science, University of Kerbala, Iraq

ARTICLE INFO

Article History:

Received 05 July 2024

Accepted 24 September 2024

Published 01 October 2024

Keywords:

Laser medium

Random laser

Rhodamine dye

Sol-gel

TiO₂

ABSTRACT

Rhodamine B dye-doped with titanium dioxide (TiO₂) nanoparticles in certain proportions were prepared by simple sol-gel technique. The structural and morphological properties of the prepared samples were studied using X-ray diffraction (XRD) and field emission scanning electron microscopy (FESEM). The results showed that the TiO₂ nanoparticles have spherical agglomerated shapes with anatase and rutile phases. The average crystallite size of the samples was calculated using the Debye-Schärer formula, ranging from (10 to 24) nm for anatase and rutile phases. The results show that when a percentage of Rhodamine is introduced, the crystallite diameter increases and the diameter ranges from (4 to 12) nm. The intensity of the peaks changes significantly and the phase is transformed by increasing the percentage of Rhodamine.

How to cite this article

Rwayyih N., Tahir K., Ridha N., Alosfur F. Study of the Structural Properties of Rhodamine Dye-Doped With TiO₂ Nanoparticles. J Nanostruct, 2024; 14(4):1287-1295. DOI: 10.22052/JNS.2024.04.028

INTRODUCTION

The use of nanomaterials in laser media represents an exciting and innovative field in materials science and technology. Due to their small size, which ranges from 1 to 100 nanometers, these materials have unique properties that distinguish them from conventional materials [1]. Nanomaterials contribute to improving the chemical, mechanical, optical, electrical, and magnetic properties of the material [2]. Titanium dioxide is one of the most prominent and important nanomaterials, as it is characterized by its high potential and excellent performance in most applications [3]. This material also has a great ability to absorb ultraviolet rays and stimulate chemical reactions, in addition to being a non-toxic, low-cost, and light-resistant material [4]. This material exists in three different crystalline

phases, which are rutile, anatase, and brookite, where the rutile phase is considered the most stable, and each phase has its own properties suitable for a variety of applications [5]. This material can be prepared in several ways, including spraying, reactive thermal deposition, chemical vapor deposition, sol-gel, and spray thermal analysis [6]. The sol-gel method is considered the most suitable due to its advantages in obtaining a homogeneous material required in applications [7]. The crystal structure of the nanomaterial can be controlled through the synthesis conditions [8]. This nanomaterial can be used with laser dye to improve the properties and apply them in certain fields such as using them in random laser media where they amplify light [9]. The laser dye is known as an organic dye with multiple applications, and one of the laser dyes is the

* Corresponding Author Email: khawla.taher@uokerbala.edu.iq



Rhodamine dye which is used in many applications due to its unique properties, as it is characterized by its ability to absorb light and re-emit it with high efficiency, in addition to its chemical stability and easy solubility [10]. Research indicates that increasing the concentration of additives [11] and the temperature used in annealing [12] can lead to changes in the crystal structure. Other studies have shown that when the dye concentration is increased, interference between molecules may occur, which negatively affects the crystal arrangement and leads to an increase in the crystal size or even a change in the crystal shape [13]. The effect of the Rhodamine dye concentration on the size of TiO₂ crystals depends largely on the ratio used and the specific application. According to studies, it is preferable to use Rhodamine dye with TiO₂ as an effective laser medium so that the dominant phase of TiO₂ is rutile [14]. Researchers Majida A. Ameen et al. 2022 studied titanium oxide (TiO₂) nanofilms prepared by sol-gel dip-coating and doped with Rhodamine 6G (R6G). The results showed that the films are amorphous and have a homogeneous surface. R6G was incorporated into TiO₂, suggesting the potential of these films for the fabrication of visible and ultraviolet lasers [15]. Researchers Noor Y Khudair, and Mohammed K Dhahir 2023 fabricated laser gain media using different dyes and silicon dioxide (SiO₂) nanoparticles using Sol-Gel technology. The results showed that the dyes doped with silica had lower absorption and higher fluorescence spectra. The analyses also showed that the silica particles were spherical with a size of 25-67 nm, making them suitable for constructing laser media [16]. Researchers Noor Y Khudair, and Mohamed K Dhahir 2024 demonstrated random laser gain media using Rhodamine 101 dye and SiO₂ nanoparticles at different concentrations. These media were fabricated using Sol-Gel technology and using a pulsed blue laser to produce random lasers, with the reflected light collected by a spectrometer. The results showed a coherent random laser at 532-536 nm, with the best maximum width at the optimum concentration. Electron microscopy showed that the SiO₂ particles were spherically packed with an average size between 25 and 52 nm. The absorption spectra of R640 dye with nanoparticles at different concentrations were also analyzed [17].

In this work, Rhodamine dye RhB doped with TiO₂ in certain ratios was prepared using the sol-

gel method. The structural and morphological properties of the samples were studied with the aim of using them as active laser media in random lasers since these lasers have unique properties such as being portable, mirrorless, and low cost compared to conventional laser systems.

MATERIALS AND METHODS

Titanium isopropoxide, a colorless to yellowish liquid, was used as the basic material for titanium oxide. In addition, Rhodamine dye, pure ethanol (Ethyl Alcohol 99.9%), hydrochloric acid (HCl, HClO₃ 36.5-38.0%), and deionized water were used.

Sample Preparation

Rhodamine B dye solution was prepared by dissolving the required amount in ethanol. Before dissolution, the weight of the dye was measured using a sensitive balance, and the weight was calculated using the following equation [18]:

$$W = (M.V.C) / 1000 \quad (1)$$

Where:

W is the weight (gm), M is the molecular weight of the dye (gm/mol), V is the volume of the solution (ml), and C is the molar concentration (M) A high concentration of the dye solution was prepared and then diluted to a concentration of (1×10^{-4} M) using the dilution law [19]:

$$C_1.V_1 = C_2.V_2 \quad (2)$$

Where:

C₁ is the initial concentration before dilution, V₁ is the initial volume before dilution, C₂ is the second diluted concentration, and V₂ is the second volume after dilution.

This solution was stored in a silicon-coated flask. Then, pure TiO₂ was prepared by adding 10 ml of TTIP (the basic material for forming TiO₂) to 50 ml of ethanol in a glass beaker. The beaker was placed on a magnetic stirrer for a quarter of an hour at 600 rpm to homogenize the components. In another beaker, 50 ml of ethanol was added with 10 ml of water and 1 ml of HCl, and these materials were homogenized, then added to the ethanol and TTIP solution, and the stirring process continued for an hour, and a gel-like substance of pure TiO₂ was obtained. Then, the ratio of 75% TiO₂ and 25% RhB was prepared, where 35 ml of ethanol

was added with 10 ml of TTIP and 15 ml of diluted dye solution. The solution was mixed and left on a magnetic stirrer at 600 rpm for a quarter of an hour. In another beaker, 10 ml of water and 1 ml of HCl

were added to 50 ml of ethanol and mixed well, then added to the mixture by distillation and left on a magnetic stirrer for an hour, which resulted in obtaining a gelatinous material containing the dye

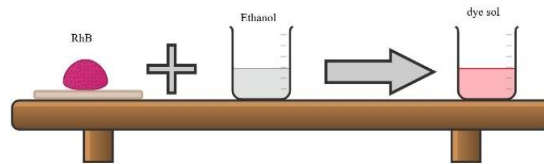
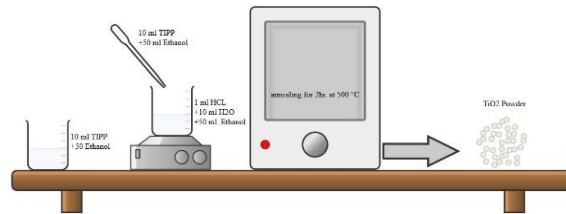
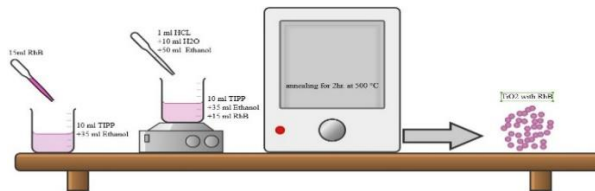


Fig. 1. Preparation of the dye.

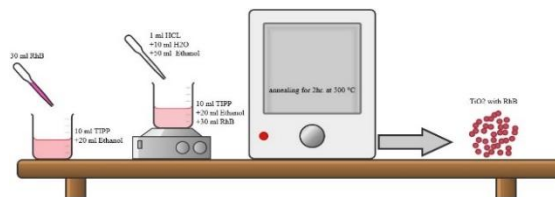
1. TiO₂ pure



2. 75%TiO₂, 25%RhB



3. 50%TiO₂, 50%RhB



4. 25%TiO₂, 75%RhB

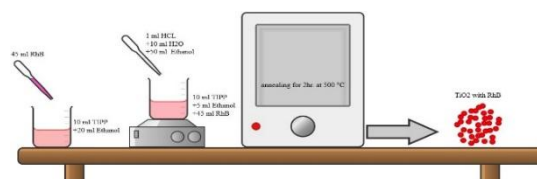


Fig. 2. Showing the preparation of TiO₂-doped Rhodamine.

impregnated with TiO₂ in the required proportion. Then we prepared the ratio of 50% TiO₂ and 50% RhB, where we added 10 ml of TTIP to 20 ml of ethanol, then added 30 ml of the dye solution prepared by distillation. We left the mixture on the magnetic stirrer for a quarter of an hour to homogenize the materials. After that, in another beaker, 50 ml of ethanol was added with 10 ml of water and 1 ml of HCl and mixed gently, then added to the solution containing TTIP, ethanol, and dye, and the stirring process continued for an hour to obtain a gelatinous solution in the required proportions. Finally, we prepared the ratio of 25% TiO₂ and 75% RhB, where 10 ml of TTIP was added to 5 ml of ethanol, then 45 ml of the prepared dye solution was added. The mixture was left on the magnetic stirrer for a quarter of an hour, and in another flask, 50 ml of ethanol, 10 ml of water, and 1 ml of HCl were added, after mixing the materials well, they were added dropwise to the solution containing the dye and TTIP. We left the mixture for a full hour on the stirrer at a speed of 600 rpm until we obtained a gelatinous solution in the required ratio. After preparing these samples, they were left in a dark place for some time until they dried, and then we ground them manually to obtain a fine powder. After grinding, these samples were placed in the oven at a temperature of 500 °C to obtain the samples after annealing. After that, the structural and morphological properties

of the Rhodamine dye were studied after doping with the nanomaterial to determine the effect of the nanomaterial on the dye (Fig. 1 and Fig. 2).

RESULTS AND DISCUSSION

X-Ray Diffraction (XRD) Analysis

Fig. 3. shows the X-ray diffraction patterns for TiO₂, 75%TiO₂-25%Rh, 50%TiO₂-50%Rh and 25% TiO₂-75%Rh; The XRD patterns of TiO₂ exhibited a peak at 2θ = 25.2°, 37.8°, 48.1°, 55.1° and 62.7° which assigned to (101), (004), (200), (211) and (204) crystal lattice planes of the anatase form in TiO₂, (JCPDS Card no. 96-900-8214) and at 2θ = 27.5°, 44.76°, 54.3°, 56.6° and 69.8° which assigned to (110), (210), (211), (220) and (301) indicated the rutile form of TiO₂ (JCPDS Card no. 96-900-4145). The intensity of these peaks at 2θ = 25.2°, 27.5°, 37.8° and 54.3° changes significantly with the introduction of different percentages of Rhodamine B, indicating the effect of the introduction of this dye in the transformation of anatase to rutile titanium dioxide phases. By increasing Rhodamine B percentage diffraction peaks from Rhodamine B (C₂₈H₃₁ClN₂O₃) could not be observed due to the interference with TiO₂ peaks, which is consistent with the findings of xiuhua et al [20].

The Tables 1, 2, 3, and 4 present the XRD results for the synthesized TiO₂ and TiO₂-RhB nanoparticles. We can observe the effect of

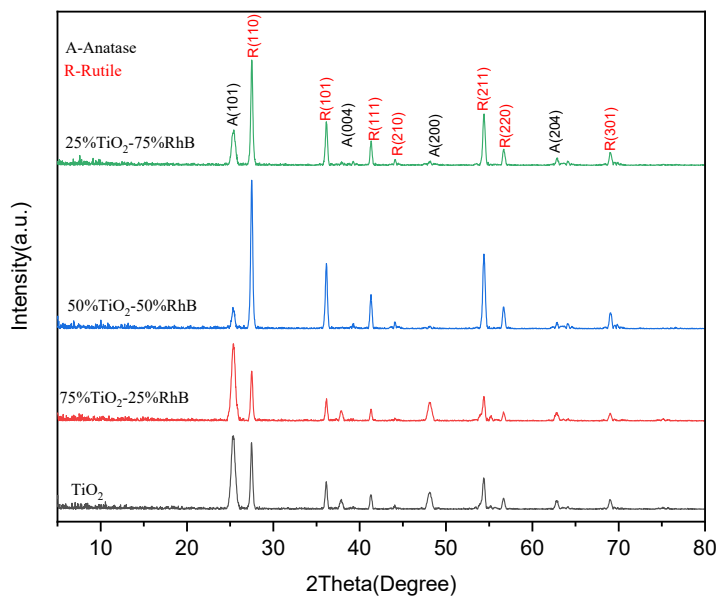


Fig. 3. XRD patterns of TiO₂ and TiO₂-RhB samples.

Rhodamine dye concentration on the crystal size where Determining the crystal size of the samples using the Debye-Scherrer formula [21].

$$D = K\lambda / \beta \cos\theta \tag{3}$$

In this equation, *D* represents the average

Table 1. XRD analysis results of sample TiO₂.

	2θ (°)	d (Å)	(h k l)	The phase	FWHM (°)	Crystalline size (nm)
1.	25.354	3.51	(1 0 1)	Anatase	0.69428	11.7283
2.	27.465	3.244	(1 1 0)	Rutile	0.34239	23.8852
3.	36.133	2.483	(1 0 1)	Rutile	0.38678	21.6047
4.	37.785	2.379	(0 0 4)	Anatase	1.26891	6.6172
5.	41.297	2.184	(1 1 1)	Rutile	0.37217	22.8112
6.	44.091	2.052	(2 1 0)	Rutile	0.4751	18.0402
7.	48.077	1.891	(2 0 0)	Anatase	0.7621	11.4141
8.	54.392	1.685	(2 1 1)	Rutile	0.53511	16.6913
9.	56.689	1.622	(2 2 0)	Rutile	0.42311	21.3336
10.	62.728	1.480	(2 0 4)	Anatase	0.71544	13.0042
Average Crystalline Size Of Anatase Phase					10.69095	
Average Crystalline Size Of Rutile Phase					20.7277	

Table 2. XRD analysis results of sample 75%TiO₂, 25%RhB.

	2θ (°)	d (Å)	(h k l)	The phase	FWHM (°)	Crystalline size (nm)
1.	25.307	3.516	(1 0 1)	Anatase	0.6379	12.7638
2.	27.508	3.239	(1 1 0)	Rutile	0.3625	22.5622
3.	36.951	2.4307	(1 0 3)	Anatase	0.3760	22.2765
4.	37.792	2.378	(0 0 4)	Anatase	0.9945	8.4432
5.	41.335	2.182	(1 1 1)	Rutile	0.3633	23.3710
6.	44.162	2.049	(2 0 1)	Rutile	0.4865	17.6219
7.	48.043	1.8922	(2 0 0)	Anatase	0.7067	12.3072
8.	54.459	1.6835	(2 1 1)	Rutile	0.6449	13.8539
9.	56.784	1.6199	(2 2 0)	Rutile	0.4107	21.9881
10.	62.689	1.4808	(2 0 4)	Anatase	0.7154	13.0023
Average Crystalline Size Of Anatase Phase					13.7586	
Average Crystalline Size Of Rutile Phase					19.87942	

Table 3. XRD analysis results of sample 50%TiO₂, 50%RhB

	2θ (°)	d (Å)	(h k l)	The phase	FWHM (°)	Crystalline size (nm)
1.	25.367	3.508	(1 0 1)	Anatase	0.8477	9.6059
2.	27.445	3.247	(1 1 0)	Rutile	0.3026	27.0248
3.	36.081	2.487	(1 0 1)	Rutile	0.3126	26.7275
4.	37.909	2.3715	(0 0 4)	Anatase	0.568	14.7882
5.	41.24	2.1871	(1 1 1)	Rutile	0.3227	26.3032
6.	44.059	2.0536	(2 1 0)	Rutile	0.4151	20.6455
7.	48.158	1.888	(2 0 0)	Anatase	0.8704	9.9970
8.	54.051	1.6952	(1 0 5)	Anatase	0.3731	23.9027
9.	56.646	1.6235	(2 2 0)	Rutile	0.3944	22.8819
10.	62.867	1.477	(2 0 4)	Anatase	0.5398	17.2483
Average Crystalline Size Of Anatase Phase					15.10842	
Average Crystalline Size Of Rutile Phase					24.71658	



crystallite size, K is a constant, which is set to 0.94 in this case, λ is the X-ray wavelength (Cu $K\alpha = 0.154056$ nm), β is the corrected band broadening

(full width at half-maximum (FWHM)), and θ is the diffraction angle.

We note that the average crystal size in TiO_2

Table 4. XRD analysis results of sample 25% TiO_2 , 75%RhB.

	2θ ($^\circ$)	d (Å)	(h k l)	The phase	FWHM ($^\circ$)	Crystalline size (nm)
1.	25.354	3.5100	(1 0 1)	Anatase	0.7970	10.2167
2.	27.465	3.244	(1 1 0)	Rutile	0.3074	26.6039
3.	36.884	2.4350	(1 0 3)	Anatase	0.3455	24.2383
4.	37.785	2.3790	(0 0 4)	Anatase	0.7350	11.4239
5.	41.297	2.1844	(1 1 0)	Rutile	0.3162	26.8489
6.	44.091	2.0522	(2 1 0)	Rutile	0.4199	20.4118
7.	48.077	1.8910	(2 0 0)	Anatase	0.7234	12.0247
8.	54.392	1.6854	(2 1 1)	Rutile	0.3992	22.3740
9.	56.689	1.6224	(2 2 0)	Rutile	0.4063	22.2163
10.	62.728	1.4800	(2 0 4)	Anatase	0.6094	15.2671

Average Crystalline Size Of Anatase Phase					14.63414
Average Crystalline Size Of Rutile Phase					23.69098

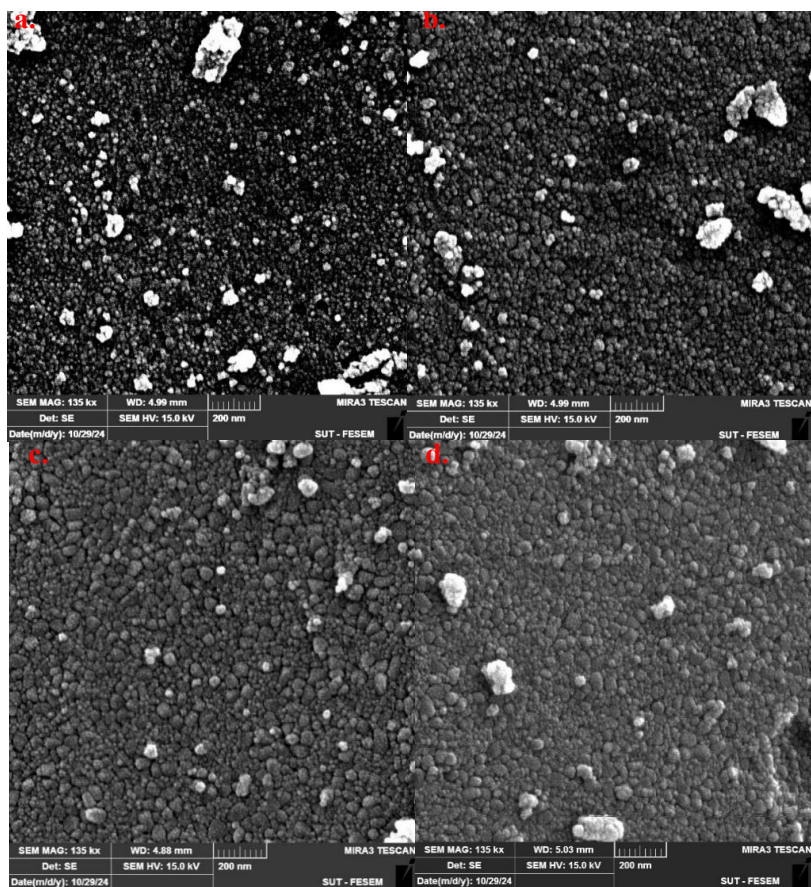


Fig. 4. The FESEM images of (a) TiO_2 , (b) 75% TiO_2 -25% RhB (c) 50% TiO_2 -50% RhB and (d) 25% TiO_2 -75% RhB samples.

only for the anatase phase is 10.69 nm and for the rutile phase is 20.73 nm. This size represents the ground state of titanium, where the crystals are in their pure state. At the ratio of 25% Rhodamine and 75% TiO₂, the average crystal size of the anatase phase was 13.76 nm and for the rutile phase, it was 19.88 nm. Here, we notice a slight change in the average crystal size, indicating that the addition of Rhodamine did not significantly affect the structure of TiO₂. This could be because the low concentration of Rhodamine did not significantly affect the crystal growth process. This ratio provides high stability because it contains a high amount of titanium, meaning it can be used in applications that require high laser energy, but with less efficiency. At the ratio of 50% Rhodamine and 50% TiO₂, the average crystal size of the anatase phase was 15.11 nm and for the rutile phase, it was 24.72 nm. We notice an increase in the crystal size here, indicating that the balanced concentration between Rhodamine and TiO₂ began

to affect the crystal structure of TiO₂. It is possible that Rhodamine contributed to enhancing the growth of the crystals or changing the way they were arranged. This ratio achieves a good balance between stability. Efficiency and this ratio are considered optimal for applications that require high efficiency. At a ratio of 75% Rhodamine and 25% TiO₂, the average crystal size of the anatase phase is 14.63 nm and the rutile phase is 23.69 nm. Although the size is still larger than in the case of TiO₂ alone, it may indicate opposite effects, as a high concentration of Rhodamine can reduce the effectiveness of crystal growth of TiO₂. This ratio increases the absorption efficiency but reduces the stability of the medium at high energies. This ratio is suitable for low-power laser applications. According to the ratios used, the low concentration may not have much effect, while the medium concentration (50%) shows a positive effect on the crystal size and on increasing the intensity in the rutile phase, and is considered the optimal

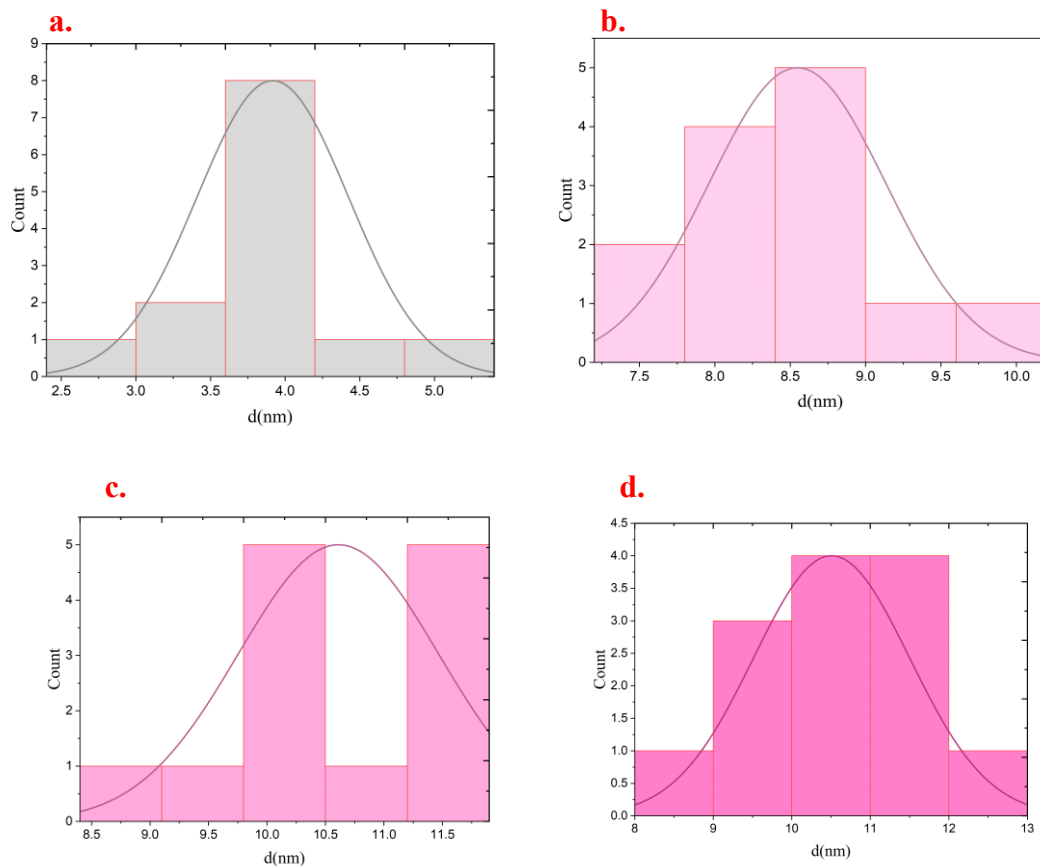


Fig. 5. The size distribution of (a) TiO₂ (b) 75% TiO₂, 25% RhB (c) 50% TiO₂, 50% RhB and (d) 25% TiO₂-75% RhB samples.

ratio to achieve a balance between efficiency and stability. However, the high concentration (75%) may lead to negative interferences, meaning that there must be a balance in using the dye with different concentrations of TiO₂ and according to the specific application.

FESEM Analysis

The morphological properties of TiO₂ and TiO₂-RhB samples were examined using field emission scanning electron microscopy (FESEM). The results of FESEM analysis are shown in Fig. 4, at a scale of 200 nm. The obtained images clearly demonstrate the porous nature of pure TiO₂ and TiO₂-RhB samples. It is worth noting that the nanoparticles exhibit a high degree of size uniformity and mainly exhibit a spherical morphology. This is consistent with researcher Sambandam Balaji [22]. Moreover, it is evident that these nanoparticles are interconnected, resulting in a disorganized porous network structure. When the concentration of Rhodamine B is increased to 75%, an increment in crystal size and agglomeration is observed.

Fig. 5 shows the particle size distribution of the samples. The data presented in the graph indicated that the calculated particle sizes of TiO₂, 75% TiO₂-25% RhB, 50% TiO₂-50% RhB, and 25% TiO₂-75% RhB samples are 4 nm, 9 nm, 10, 11 nm, and 12 nm. Rhodamine B, a fluorescent dye, may affect the formation and growth processes of TiO₂ crystals. The dye may interact with TiO₂, resulting in differences in particle size, shape, and distribution this is consistent with researcher Neyda Bager [23]. It is worth noting that the sol-gel method greatly affects the structural properties of TiO₂, resulting in the agglomeration of particles and the formation of irregular shapes this is consistent with [24,25].

CONCLUSION

The optimal ratio selection for titanium and Rhodamine dye as a laser medium depends on laser properties. The structural and morphological properties were studied using XRD and FESEM analysis of samples prepared with different ratios of Rhodamine dye-doped with nano-TiO₂ material. The results showed that the ratio of 50%TiO₂ and 50% Rhodamine dye positively affects the crystal size and increases the intensity in the rutile phase. This ratio is also considered the optimal ratio to achieve a balance between efficiency and stability. However, when the titanium ratio increases to

75% TiO₂ and 25% Rhodamine, it increases the energy loss due to dispersion. At a lower ratio of titanium, i.e. at a ratio of 25% TiO₂ and 75% Rhodamine, it reduces the stability of the medium at high energies. As shown by the analysis of the FESEM results, the diameter of the crystals in the ratio of 50% TiO₂ and 50% Rhodamine is from 10 to 11 nanometers.

ACKNOWLEDGMENTS

We extend our sincere thanks and gratitude to the University of Kerbala for the support it provided, which contributed to the completion of this research.

CONFLICT OF INTEREST

The authors declare that there is no conflict of interests regarding the publication of this manuscript.

REFERENCES

- Haider A, Kang I-K. Preparation of Silver Nanoparticles and Their Industrial and Biomedical Applications: A Comprehensive Review. *Advances in Materials Science and Engineering*. 2015;2015:1-16.
- Li B, Wang X, Yan M, Li L. Preparation and characterization of nano-TiO₂ powder. *Materials Chemistry and Physics*. 2003;78(1):184-188.
- Wang Y, He Y, Lai Q, Fan M. Review of the progress in preparing nano TiO₂: An important environmental engineering material. *Journal of Environmental Sciences*. 2014;26(11):2139-2177.
- Nakata K, Fujishima A. TiO₂ photocatalysis: Design and applications. *Journal of Photochemistry and Photobiology C: Photochemistry Reviews*. 2012;13(3):169-189.
- Hu Y, Tsai HL, Huang CL. Phase transformation of precipitated TiO₂ nanoparticles. *Materials Science and Engineering: A*. 2003;344(1-2):209-214.
- Neama RJ, Alosfur FKM, Tahir KJ, Ridha NJ, Ahmed LM. Preparation of Au-Doped Two-Phase TiO₂ Nanoparticles by One-Step Method as Photocatalytic Applications. *Indonesian Journal of Chemistry*. 2024;24(4):1117.
- Liqiang J, Xiaojun S, Weimin C, Zili X, Yaoguo D, Honggang F. The preparation and characterization of nanoparticle TiO₂/Ti films and their photocatalytic activity. *Journal of Physics and Chemistry of Solids*. 2003;64(4):615-623.
- Mohamad Alosfur FK, Ridha NJ, Jumali MHH, Radiman S. One-step formation of TiO₂ hollow spheres via a facile microwave-assisted process for photocatalytic activity. *Nanotechnology*. 2018;29(14):145707.
- Chiad BT, Latif KH, Kadhim FJ, Hammed MA. Random Laser of R6G Dye and TiO₂ Nanoparticles Doped in PMMA Polymer. *Advances in Materials Physics and Chemistry*. 2011;01(02):20-25.
- On C, Tanyi EK, Harrison E, Noginov MA. Effect of molecular concentration on spectroscopic properties of poly(methyl methacrylate) thin films doped with rhodamine 6G dye. *Optical Materials Express*. 2017;7(12):4286.

11. Kitur J, Zhu G, Bahoura M, Noginov MA. Dependence of the random laser behavior on the concentrations of dye and scatterers. *Journal of Optics*. 2010;12(2):024009.
12. Alijani M, Ilkhechi NN. Effect of Ni Doping on the Structural and Optical Properties of TiO₂ Nanoparticles at Various Concentration and Temperature. *Silicon*. 2018;10(6):2569-2575.
13. Drexhage KH. 5. Structure and properties of laser dyes. *Topics in Applied Physics: Springer Berlin Heidelberg*; 1973. p. 155-200.
14. Noginov MA, Zhu G, Fowlkes I, Bahoura M. GaAs random laser. *Frontiers in Optics 2004/Laser Science XXII/Diffractive Optics and Micro-Optics/Optical Fabrication and Testing: OSA*; 2004. p. FTuG1.
15. Ameen MA, Saeed MA, Mahmood AS. Dip-coating sol-gel preparation and characterization of Rhodamine 6G-doped nanostructured TiO₂ thin films on structural and spectroscopic properties. *Journal of Sol-Gel Science and Technology*. 2022;101(3):655-671.
16. Noor YK, Mohammed KD. Study the Impact of Silica Nanoparticles on the Properties of Several Dyes for the Fabrication of a Random Laser Gain Medium. *Iraqi Journal of Laser*. 2023;22(2):63-70.
17. Khudair NY, Dahir MK. Fabrication of a random laser gain medium using Rhodamine 101 dye doped with SiO₂ nanoparticles by Sol-Gel technique. *Optics & Laser Technology*. 2024;169:110185.
18. Al-Hamdani AH. Studying the spectral properties of thin films of rhodamine (6G) dyes doped polymer (PMMA) dissolved in chloroform. *Iraqi Journal of Physics*. 2019;12(23):59-64.
19. Hameed AS, Ridha NJ, Madloul RA, Alosfurb FKM, Tahir KJ. Influence of growth acidic solution and etching time on rutile TiO₂ nanorod arrays synthesized by hydrothermal method in dye-sensitized solar cells. *Digest Journal of Nanomaterials and Biostructures*. 2022;17(4):1353-1367.
20. Xiu-hua L, Dan M, Yi D. Effects of Rhodium Doping on the Microstructures and Photocatalytic Performances of TiO₂ Powders. *Journal of Chemical Research*. 2016;40(11):678-682.
21. Zhang J, Gao L. Synthesis and characterization of nanocrystalline tin oxide by sol-gel method. *J Solid State Chem*. 2004;177(4-5):1425-1430.
22. Sambandam B, Surendran A, Philip L, Pradeep T. Rapid Synthesis of C-TiO₂: Tuning the Shape from Spherical to Rice Grain Morphology for Visible Light Photocatalytic Application. *ACS Sustainable Chemistry & Engineering*. 2015;3(7):1321-1329.
23. Baguer N, Georgieva V, Calderin L, Todorov IT, Gils SV, Bogaerts A. Study of the nucleation and growth of TiO₂ and ZnO thin films by means of molecular dynamics simulations. *Journal of Crystal Growth*. 2009;311(16):4034-4043.
24. Heshmatpour F, Aghakhanpour RB. Synthesis and characterization of superfine pure tetragonal nanocrystalline sulfated zirconia powder by a non-alkoxide sol-gel route. *Adv Powder Technol*. 2012;23(1):80-87.
25. Kadhim HBA, Ridha NJ, Mohamad Alosfur FK, Umran NM, Madloul R, Tahir KJ, et al. Ablation of ZnO in liquid by Nanosecond Laser. *Journal of Physics: Conference Series*. 2018;1032:012039.